



Calculation of Unsaturated Seismic Active Earth Pressure under Steady-State Seepage Conditions

Ranran Song¹, Junguo Peng^{2*}

School of Civil Engineering, Lanzhou University of Technology, Gansu, China

¹First author's e-mail:1628563431@qq.com

^{2*} Corresponding author's e-mail address:
pengjg@lut.edu.cn

Abstract. In order to improve the calculation method of soil pressure on retaining walls under earthquake action, a calculation formula for seismic active soil pressure on unsaturated retaining walls under steady-state seepage conditions was derived based on the variational method and limit equilibrium method. The rationality of the formula in this paper was verified by comparing the calculated values with existing results. And the influence of fitting parameters and seismic coefficients on the active earth pressure coefficient was analyzed through numerical calculations in Matlab. The results showed that the active earth pressure coefficient decreased with the decrease of fitting parameter α value and gradually approached a fixed value; The increase in both vertical and horizontal seismic coefficients will lead to an increase in the active earth pressure coefficient. The research results have certain reference value for the development of unsaturated seismic active earth pressure.

Keywords: Active earth pressure; Seismic coefficient; Steady-state flow; Variational method

1 INTRODUCTION

As a supporting structure to prevent deformation and destabilization of the soil behind the wall, retaining walls are widely used in perimeter slope support projects such as housing construction, railroads and highways. In the design of retaining wall, accurate calculation of the magnitude of earth pressure is the core factor of retaining wall design, and it is also one of the important research topics in the field of geotechnical engineering. In recent years, domestic and foreign scholars have conducted research on the calculation of saturated soil pressure through different methods. However, in practical engineering, the fill behind retaining walls is usually unsaturated soil located above the groundwater level. Therefore, researchers are committed to finding and determining more accurate methods for calculating soil pressure. Vahedifard et al.^[1] (2015) explored the active earth pressure problem of unsaturated soils under steady state seepage conditions, utilizing the effective stress concept proposed by Lu et al.^[2] (2006) and combining it with the Gardner equation to simulate one-dimensional steady state seepage,

and then deriving the corresponding expression for active earth pressure. In addition, the key parameters affecting the active earth pressure are investigated through numerical analysis. Peng et al. [3] (2023) calculated the active and passive soil pressures of unsaturated soil under transient seepage, and conducted numerical analysis on the main parameters affecting soil pressure.

The proposed static method for calculating earth pressures under earthquakes is widely used. Zhang[4] (2014) used the rotation angle method to transform the active earth pressure calculation under seismic action into the active earth pressure solution problem under static conditions, and used the existing static equations to give the distribution of earth pressure strength and the location of the point of action when the fill surface is inclined. Morrison et al. [5] (1995) used the limit equilibrium method to calculate passive earth pressures under seismic action, where the slip surface was assumed to be a logarithmic spiral slip surface. The above calculation of soil pressure under seismic conditions is only applicable to saturated soils.

Previous studies on seismic earth pressures in unsaturated soils under steady state seepage conditions have been inadequate. In this paper, the logarithmic helix slip surface equation is obtained based on the variational principle, and the limit equilibrium equation is constructed, so as to derive the formula for calculating the seismic active earth pressure of unsaturated soils under steady state seepage conditions. The calculated results were compared with the existing ones, and numerical calculations were carried out using Matlab software to explore the effects of fitting parameters and seismic coefficients on the active earth pressure coefficients.

2 THEORETICAL STUDIES

Effective stress and shear strength of unsaturated soils:

$$\sigma' = \sigma - u_a - \sigma^s \tag{1}$$

$$\sigma^s = -(u_a - u_w) \quad (u_a - u_w) \leq 0 \tag{2}$$

$$\sigma^s = -\frac{(u_a - u_w)}{\{1 + [\alpha(u_a - u_w)]^n\}^{(n-1)/n}} \quad (u_a - u_w) > 0 \tag{3}$$

Where σ = total stress; σ' = effective stress; u_a = pore-air pressure; u_w = pore-water pressure; $(u_a - u_w)$ = matric suction; and α and n = fitting parameter.

Using the Mohr–Coulomb criterion, the shear strength is expressed as follows:

$$\tau = c' + \sigma' \tan \phi' \tag{4}$$

where τ = shear strength at failure; c' = effective cohesion; ϕ' = Effective internal friction angle.

Gardner’s obtained an analytical solution for solving unsaturated seepage by means of soil-water characteristic curves for unsaturated soils:

$$K_* = K_s e^{-\alpha \gamma_w h_m} \tag{5}$$

Where K_s = saturated hydraulic conductivity; K^* = unsaturated hydraulic conductivity; h_m = suction head.

If the boundary conditions are set at the water table it can be obtained that an analytical solution for the one-dimensional suction can be obtained:

$$(u_a - u_w) = -\frac{1}{\alpha} \ln\left[\left(1 + \frac{q}{K_s}\right)e^{-\alpha\gamma_w z} - \frac{q}{K_s}\right] \tag{6}$$

where q = Vertical flow rate per unit area; γ_w = Unit weight of water; z = Vertical height above water surface.

Substituting Eq. (6) into Eq. (3) yields:

$$\sigma^s = \frac{1}{\alpha} \frac{\ln\left[\left(1 + \frac{q}{K_s}\right)e^{-\alpha\gamma_w z} - \frac{q}{K_s}\right]}{\left(1 + \left\{-\ln\left[\left(1 + \frac{q}{K_s}\right)e^{-\alpha\gamma_w z} - \frac{q}{K_s}\right]\right\}^n\right)(n-1) / n} \tag{7}$$

Eq. (7) is applied to the formulation of lateral earth pressures incorporating a log spiral failure mechanism. σ^s = suction stress

3 ACTIVE EARTH PRESSURE FORMULATIONS

The active soil pressure analysis model is shown in Fig. 1, which q is the uniform surcharge (kN/ m), k_v is vertical seismic coefficient, k_h is horizontal seismic coefficient (The direction and sign are specified as $k_h[\leftarrow-], k_v[\downarrow+, \uparrow-]$), H is the height of the wall with an angle ω between the wall facing and the vertical axis, β is the backfill inclination, δ is the soil-facing interface friction angle, P_a is the combined force of active earth pressures, $y(x)$ is slip surface function, y_0 is the depth to the water table below the toe of the wall. θ_0 and θ_1 are the polar angles of points 0 and 1. Similar to the approach taken by Baker and Garber^[6] (1978) by using the geometrical relations $\cos \bar{\gamma} = dx / dl$; $\sin \bar{\gamma} = ydx / dl$ (Fig. 1), The equilibrium equations of horizontal and vertical forces and moments around the origin can be written as follows:

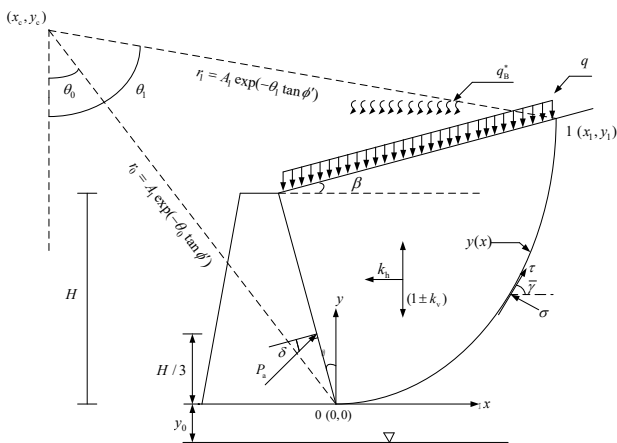


Fig. 1. Active earth pressure analysis model

$$\begin{aligned}
 & P_a \cos(\delta + \omega) - k_h(qH \tan \omega + \frac{1}{2} \gamma \tan \omega H H_1) \\
 & = \int_0^{x_1} [\sigma'(y - \tan \phi') - c' + (u_a + \sigma^s) \dot{y}] dx + \int_0^{x_1} k_h[\gamma(x \tan \beta + H_1 - y) + q] dx
 \end{aligned}
 \tag{8}$$

$$\begin{aligned}
 & P_a \sin(\delta + \omega) - (1 \pm k_v)[qH \tan \omega + \frac{1}{2} \gamma \tan \omega H H_1] \\
 & = (1 \pm k_v) \int_0^{x_1} \gamma(x \tan \beta + H_1 - y) + q dx - \int_0^{x_1} [\sigma'(1 + \dot{y} \tan \phi') + c' \dot{y} + u_a + \sigma^s] dx
 \end{aligned}
 \tag{9}$$

$$\begin{aligned}
 & \frac{H}{3} P_a \cos(\delta + \omega) + \frac{H}{3} P_a \sin(\delta + \omega) \tan \omega - k_h(qH^2 \tan \omega + \frac{1}{3} \gamma \tan \omega H^2 H_1) \\
 & - \frac{1}{2} (1 \pm k_v)[qH^2 \tan^2 \omega + \frac{1}{3} \gamma \tan^2 \omega H^2 H_1] \\
 & = \int_0^{x_1} [y(\dot{y} - \tan \phi') \sigma' + x \sigma'(1 + \dot{y} \tan \phi') + (u_a + \sigma^s)(y \dot{y} + x) + c'(xy - y)] dx \\
 & - (1 \pm k_v) \int_0^{x_1} qx + \gamma(x \tan \beta + H_1 - y) x dx + k_h \int_0^{x_1} qH + \gamma y(x \tan \beta + H_1 - y) dx
 \end{aligned}
 \tag{10}$$

where \$H_1 = H(1 + \tan \omega \tan \beta)\$; and \$\gamma\$ = unit weight of soil.

Normally, the pore air pressure is set as \$u_a = 0\$. Using Eq. (8) to define \$P_a\$ while considering Eqs. (9) and (10) as constraints, Baker and Garber (1978) showed that this problem is equivalent to the minimisation of the auxiliary function \$F\$:

$$F = \int_0^{x_1} f dx \tag{11}$$

$$f = L_0 + \lambda_1 L_1 + \lambda_2 L_2 \tag{12}$$

where

$$L_0 = [(\dot{y} - \tan \phi')\sigma' - c' + \sigma^s \dot{y}] + k_h[\gamma(x \tan \beta + H_1 - y) + q] \tag{13}$$

$$L_1 = (1 \pm k_v)[q + \gamma(x \tan \beta + H_1 - y)] - [(1 + \dot{y} \tan \phi')\sigma' + c'\dot{y} + \sigma^s] \tag{14}$$

$$L_2 = y(\dot{y} - \tan \phi')\sigma' + x(1 + \dot{y} \tan \phi')\sigma' + \sigma^s(y\dot{y} + x) + c'(x\dot{y} - y) - (1 \pm k_v)[qx + \gamma(x \tan \beta + H_1 - y)x] + k_h[qH + \gamma y(x \tan \beta + H_1 - y)] \tag{15}$$

where λ_1 and λ_2 = Lagrange undetermined multipliers.

According to the Euler differential equations for function f :

$$\frac{\partial f}{\partial \sigma'} = \frac{d}{dx} \frac{\partial f}{\partial \dot{\sigma}'} \tag{16}$$

$$\frac{\partial f}{\partial y} = \frac{d}{dx} \frac{\partial f}{\partial \dot{y}} \tag{17}$$

Since f is independent of $\dot{\sigma}'$, Eq. (16) yields:

$$\frac{\partial f}{\partial \sigma'} = 0 \tag{18}$$

substituting Eq. (12) into Eq. (18):

$$\frac{dy}{dx} = \frac{\tan \phi'(1 / \lambda_2 + y) + (\lambda_1 / \lambda_2 - x)}{\tan \phi'(x - \lambda_1 / \lambda_2) + (1 / \lambda_2 + y)} \tag{19}$$

where $\lambda_2 \neq 0$. Eq. (19) can be simplified by the following polar coordinate transformation:

$$y + 1 / \lambda_2 = -r \cos \theta \tag{20}$$

$$x + \lambda_1 / \lambda_2 = r \sin \theta \tag{21}$$

where $x_c = -\lambda_1 / \lambda_2$; $y_c = -1 / \lambda_2$; (r, θ) = coordinates in the polar coordinate system.

The coupled equations (19), (20) and (21) yield:

$$r = A_1 \exp(-\theta \tan \phi') \tag{22}$$

Bringing the coordinates of points 0 and 1 into equations (20) and (21) yields:

$$A_1 = \frac{H_1}{e^{(-\theta_0 \tan \phi')}(\cos \theta_0 + \sin \theta_0 \tan \beta) - e^{(-\theta_1 \tan \phi')}(\cos \theta_1 + \sin \theta_1 \tan \beta)} \tag{23}$$

where A_1 is the constant of integration associated with the position of the pole (x_c, y_c) .

Baker and Garber (1978) proved that the minimisation of the auxiliary function F is equivalent to a moment balance equation for the poles. The moment balance equation around the pole can be written as follows:

$$\begin{aligned}
 & P_a \cos(\delta + \omega)(r_0 \cos \theta_0 - \frac{H}{3}) + P_a \sin(\delta + \omega)(r_0 \sin \theta_0 - \frac{H}{3} \tan \omega) \\
 &= (1 \pm k_v)[qH \tan \omega(r_0 \sin \theta_0 - \frac{H}{2} \tan \omega) + \frac{1}{2} \gamma HH_1 \tan \omega(r_0 \sin \theta_0 - \frac{H}{3} \tan \omega)] \\
 &+ k_h[qH \tan \omega(r_0 \cos \theta_0 - H) + \frac{1}{2} \gamma HH_1 \tan \omega(r_0 \cos \theta_0 - \frac{2H}{3})] \\
 &- \int_0^{x_1} \sigma'[(\dot{y} - \tan \phi')(y - y_c) + (x - x_c)(1 + \dot{y} \tan \phi')] dx \\
 &- \int_0^{x_1} \{c'[\dot{y}(x - x_c) - (y - y_c)] + \sigma^s[\dot{y}(y - y_c) + (x - x_c)]\} dx \\
 &+ (1 \pm k_v) \int_0^{x_1} q(x - x_c) dx + \int_0^{x_1} \gamma[(x - x_c) \tan \beta + H_1 - y_c - (y - y_c)](x - x_c) dx \\
 &- k_h \int_0^{x_1} q(H - y_c) + \gamma[(x - x_c) \tan \beta + H_1 - y_c - (y - y_c)](y - y_c) dx
 \end{aligned} \tag{24}$$

The balanced equation (24) can be rewritten in the polar coordinate system as follows:

$$\begin{aligned}
 & P_a \cos(\delta + \omega)(r_0 \cos \theta_0 - \frac{H}{3}) + P_a \sin(\delta + \omega)(r_0 \sin \theta_0 - \frac{H}{3} \tan \omega) \\
 &= (1 \pm k_v)[qH \tan \omega(r_0 \sin \theta_0 - \frac{1}{2} H \tan \omega) + \frac{1}{2} \gamma HH_1 \tan \omega(r_0 \sin \theta_0 - \frac{H}{3} \tan \omega)] \\
 &+ k_h[qH \tan \omega(r_0 \cos \theta_0 - H) + \frac{1}{2} \gamma HH_1 \tan \omega(r_0 \cos \theta_0 - \frac{2H}{3})] \\
 &- \int_{\theta_0}^{\theta_1} r^2 [c' - \sigma^s \tan \phi' - (1 \pm k_v)q \sin \theta (\cos \theta - \tan \phi' \sin \theta)] d\theta \\
 &+ (1 + k_h) \int_{\theta_0}^{\theta_1} r^2 [\gamma \sin \theta (\cos \theta - \tan \phi' \sin \theta) (r \sin \theta \tan \beta + H_1 - r_0 \cos \theta_0 + r \cos \theta)] d\theta \\
 &+ k_h \int_{\theta_0}^{\theta_1} r q (r_0 \cos \theta_0 - H) (\cos \theta - \tan \phi' \sin \theta) d\theta
 \end{aligned} \tag{25}$$

According to the classical earth pressure expression, the active earth pressure P_a can be expressed as:

$$P_a = \frac{1}{2} K_a \gamma H^2 \tag{26}$$

where K_a = active earth pressure coefficient; P_a = active earth pressure.

4 COMPARISON AGAINST EXISTING ANALYTICAL SOLUTIONS

To ensure the correctness of the calculations in this paper, the results will be analysed in comparison with the results of the Vahedifard et al. (2015) study. The parameters are selected as: $H = 4 \text{ m}$, $K_s = 9 \times 10^{-7} \text{ m/s}$, $\omega = 0$, $k_v = k_h = 0$, $q = 0$, $\delta/\phi' = 0$, $\phi' = 30^\circ$, $\alpha = 0.05 \text{ kPa}^{-1}$, $c' = 1.7 \text{ kPa}$, $q_B^* = -3.14 \times 10^{-8} \text{ m/s}$, $\gamma = 20 \text{ kN/m}^3$, the results are shown in Fig. 2 Typical hydrological parameters in reference to Table 1. (Quoted from Unsaturated Soil Mechanics textbook pages 198)

Table 1. Typical hydrological parameters of sandy and clayey soils

Type of soil	n (dimensionless)	$\alpha(\text{kPa}^{-1})$	K_s (m/s)
Sand	4~8.5	0.1~0.5	$10^{-2} \sim 10^{-5}$
Silt	2~4	0.01~0.1	$10^{-6} \sim 10^{-9}$
Clay	1.1~2.5	0.001~0.01	$10^{-8} \sim 10^{-13}$

Fig. 2 shows the relationship curve between pore size distribution parameters n and active earth pressure coefficients in silt. As can be seen from Fig. 2, the calculations in this paper show a high degree of agreement with the results of Vahedifard et al.(2015) study. In addition, as n increases, the active soil pressure coefficient gradually increases, which is attributed to an increase in the proportion of larger pores in the soil, a decrease in the indirect contact surface of particles, and a decrease in shear strength.

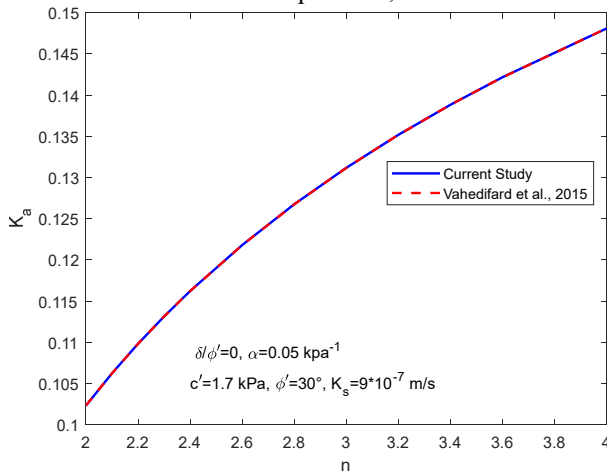


Fig. 2. Relationship between n and active earth pressure coefficient

5 PARAMETRIC STUDY

In the van Genuchten model, the parameters n and α are the key fitting parameters describing the soil-water characteristic curve. Fig. 3 shows the curve of active earth pressure coefficient versus n . The parameters are chosen as follows: $q_B^* = 0$, $q = 0$, $c' / \gamma H = 0.05$, $\omega = 0^\circ$, $k_v = k_h = 0$, $\beta = 0^\circ$.

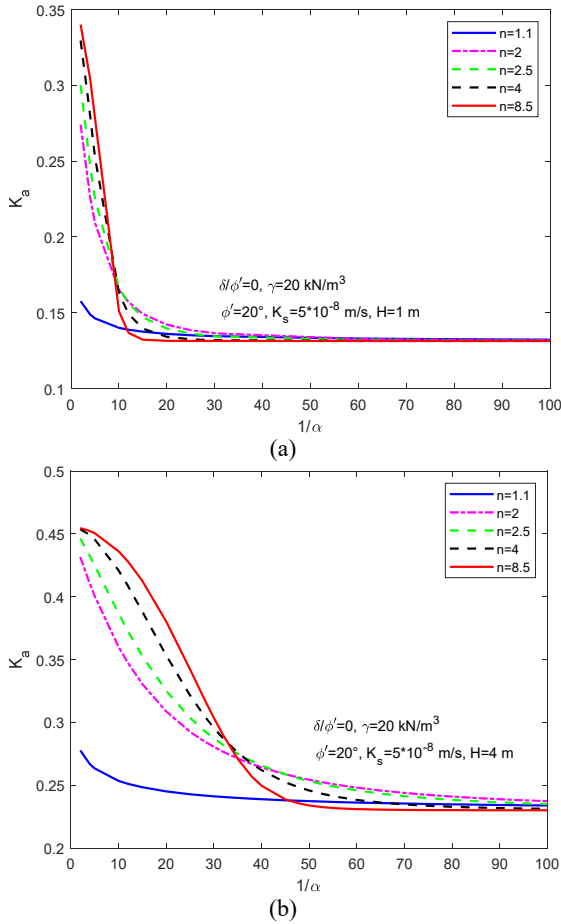


Fig. 3. Relationship between active earth pressure coefficient and n
 (a) $H = 1 \text{ m}$; (b) $H = 4 \text{ m}$

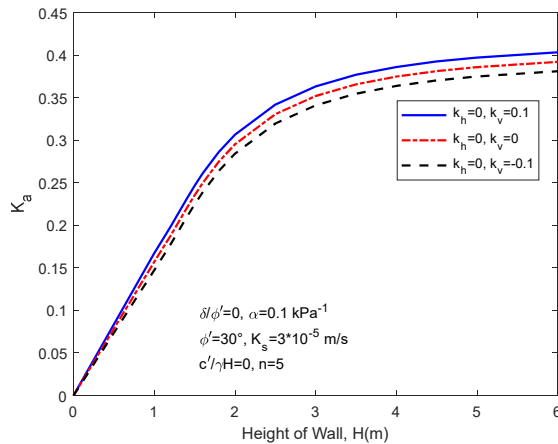
As can be seen in Fig. 3(a), the active earth pressure coefficient decreases with decreasing α value and tends to a fixed value for different n values. This indicates that the effect of substrate suction on the active earth pressure coefficient is no longer significant. Comparing Fig. 3(a) and 3(b) reveals that taller walls require a lower α value for the active earth pressure coefficient to approach a constant value. This suggests that

changes in matrix suction have a small effect on the active earth pressure coefficient at low α values.

In order to analyse the effect of seismic coefficients on active earth pressure, sandy soil is selected as the soil material and the corresponding parameters and the sign of seismic coefficients are specified as: $k_h[\leftarrow +, \rightarrow -]$, $k_v[\downarrow +, \uparrow -]$, $\phi' = 30^\circ$, $\alpha = 0.1 \text{ kPa}^{-1}$, $q = 0 \text{ kN/m}$, $\gamma = 20 \text{ kN/m}^3$, $q_B^* = -3.14 \times 10^{-8} \text{ m/s}$, $c' = 0 \text{ kPa}$, $\delta / \phi' = 0$, $n = 5$, $\beta = 0$, $K_s = 3 \times 10^{-5} \text{ m/s}$, $\omega = 10^\circ$.

Fig. 4(a) shows the trend between the vertical seismic coefficient and the active earth pressure coefficient. When the horizontal seismic coefficient is 0, the active earth pressure coefficient increases with the increment of the vertical seismic coefficient, thus for safety, the vertically downward seismic coefficient should be considered in the calculation of active earth pressure. When the wall height is 6m and the vertical seismic coefficient is increased from 0 to 0.1, the increase in the active earth pressure coefficient is 2.88%. Under seismic activity, the active earth pressure on the lower part of a retaining wall increases significantly, which causes the point of application of the resultant earth pressure to move downward. Consequently, in the seismic design of retaining walls, consideration should be given to increasing the cross-sectional size of the lower part of the wall to enhance structural stability and safety.

Fig. 4(b) shows the trend between horizontal seismic coefficients and active earth pressure coefficients. When the vertical seismic coefficient is 0.1, the active earth pressure coefficient rises with an increase in the horizontal seismic coefficient. When the wall height is 6m and the horizontal seismic coefficient is increased from 0 to 0.1, the increase in the active earth pressure coefficient is 11.21%. Comparing Fig. 4(a) and 4(b), the influence of the horizontal seismic coefficient on the active earth pressure is greater than that of the vertical seismic coefficient, due to the direct generation of horizontal acceleration in the soil by the horizontal seismic action, which increases the soil's horizontal thrust against the retaining wall. In summary, adopting a horizontal seismic coefficient directed towards the retaining wall is prudent for safety in design and calculation.



(a)

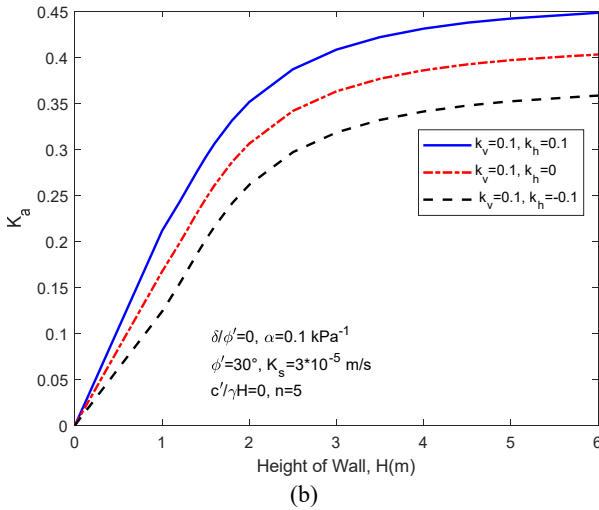


Fig. 4. Relationship between seismic coefficients and active earth pressure coefficients
 (a) $k_h = 0$; (b) $k_v = 0.1$

6 CONCLUSIONS

The formula for calculating the active earth pressure of unsaturated earth quake under steady state seepage condition is derived by the variational method combined with the limit equilibrium method. The main parameters are analyzed by numerical analysis and the results are as follows:

(1) The active earth pressure coefficient decreases with the reduction of α value and gradually tends towards a constant value. However, higher walls require a smaller α value for the active earth pressure coefficient to approximate a fixed number.

(2) Take sandy soil in the seismic intensity zone of 7 degrees for example, the active earth pressure coefficient increases with the increase of vertical and horizontal seismic coefficients. In practical engineering design, to ensure safety, it is advisable to adopt a vertically downward seismic coefficient and a horizontal seismic coefficient directed towards the retaining wall. In addition, the horizontal seismic coefficient has a more significant impact on active soil pressure.

(3) Overall, the study of soil pressure in this article has significant value in improving the safety of retaining structures, improving engineering design, and promoting theoretical development.

REFERENCES

1. Vahedifard, F., Leshchinsky, B. A., Mortezaei, K., and Lu, N. (2015) Active earth pressures for unsaturated retaining structures. *J. Geotech. Geoenviron. Eng.*, 141(11): 04015048. [https://doi.org/10.1061/\(ASCE\)GT.1943-5606.0001356](https://doi.org/10.1061/(ASCE)GT.1943-5606.0001356).

2. Lu, N., Likos, W. J. (2006) Suction stress characteristic curve for unsaturated soil. *J. Geotech. Geoenviron. Eng.*, 132(2): 131-142. [https://doi.org/10.1061/\(ASCE\)1090-0241\(2006\)132:2\(131\)](https://doi.org/10.1061/(ASCE)1090-0241(2006)132:2(131)).
3. Peng, J., Vahedifard, F. (2023) Passive and active earth pressures in unsaturated soils under transient flow using a curved failure mechanism. *J. Int. J. Geomech.*, 23(7): 04023087. <https://doi.org/10.1061/IJGNALGMENG-8085>.
4. Zhang, G. X. (2014) New analysis method of seismic active earth pressure and its distribution on a retaining wall. *J. R. S. Mech.*, 35(2):334-338+345. <https://doi.org/10.16285/j.rsm.2014.02.006>.
5. Morrison, Jr. E. E., Ebeling, R. M. (1995) Limit equilibrium computation of dynamic passive earth pressure. *J. Can. Geotech. J.*, 32(3): 481-487. <https://doi.org/10.1139/t95-050>.
6. Baker, R., Garber, M. (1978) Theoretical analysis of the stability of slopes. *J. Geotechnique*, 28(4): 395-411. <https://doi.org/10.1680/geot.1978.28.4.395>.

Open Access This chapter is licensed under the terms of the Creative Commons Attribution-NonCommercial 4.0 International License (<http://creativecommons.org/licenses/by-nc/4.0/>), which permits any noncommercial use, sharing, adaptation, distribution and reproduction in any medium or format, as long as you give appropriate credit to the original author(s) and the source, provide a link to the Creative Commons license and indicate if changes were made.

The images or other third party material in this chapter are included in the chapter's Creative Commons license, unless indicated otherwise in a credit line to the material. If material is not included in the chapter's Creative Commons license and your intended use is not permitted by statutory regulation or exceeds the permitted use, you will need to obtain permission directly from the copyright holder.

